Rapid Kinetic Studies and Structural Determination of a Cysteine Proteinase Mutant Imply That Residue 158 in Caricain Has a Major Effect upon the Ability of the Active Site Histidine To Protonate a Dipyridyl Probe[†]

Nikolaos A. Katerelos and Peter W. Goodenough*

Plant Science Laboratories, School of Plant Sciences, The University of Reading, Whiteknights, Reading RG6 6AS, U.K.

Received April 19, 1996; Revised Manuscript Received September 16, 1996[⊗]

ABSTRACT: Cysteine proteinases are endopeptidases whose catalytic activity depends upon the nucleophilicity of the active site cysteine thiol group. An ion pair forms with an active site histidine. The presence in some cysteine proteinases of an aspartic acid close to the ion pair has been used as evidence of a "catalytic triad" as found in the serine proteinases. In these enzymes, the correct alignment of serine, histidine, and aspartate residues controls catalysis. However, the absence of the homologous aspartate residue in the mammalian cysteine proteinases cathepsins B and H argues against this pivotal role for aspartic acid. Instead, an Asn, physically close to the histidine in cysteine proteinases, has been proposed as a member of the catalytic triad. Protein engineering is being used to investigate these questions. In this study, the Asp158Glu mutant of the plant cysteine proteinase caricain was analyzed by stopped-flow rapid kinetics. The probe that was used was 2,2′-dipyridyl disulfide (2 PDS), and the profile of *k* versus pH gave results more closely allied to a small molecule active site model than the normal profile with cysteine proteinases. Multiple pK_a's identified in the profile are as follows: pK_1 = 3.4 (Cys 25), pK_2 = 3.6, pK_3 = 7.0, and pK_4 = 8.6 (His 158). The structure of the enzyme with the bound inhibitor E64 was solved (*R* factor of 19.3%). Although the distance between the imadazolium and the surrounding charged amino acids is only slightly changed in the mutant, the reduced steady state activity and narrower pH range can be related to changes in the hydrogen-bonding capacity of the imadazolium.

Cysteine endopeptidases are of great biological importance and are found in all eukaryotes, bacteria, and viruses (Rawlings & Barrett, 1994). Papain has been the primary source of experimental data in the superfamily; it also has extensive industrial and medical uses. As one of the first enzyme structures to be determined through X-ray crystallography (Drenth *et al*., 1968; Pickersgill *et al.*, 1992), papain has been used in molecular replacement solutions for other members of the subfamily, namely actinidin (Baker *et al.*, 1980), calotropin DI (Heinmann *et al.*, 1982), caricain (also known as ppΩ; Pickersgill *et al*., 1991), glycyl endopeptidase (also known as pp*IV*; O'Hara *et al*., 1995) from plant origin, cruzain from *Trypanosoma cruzi* (McGrath *et al*., 1995), and liver cathepsin B (Musil *et al.*, 1991) from mammalian origin. Although these enzymes have homologous tertiary folds, other cysteine proteinases with a conserved catalytic ion pair but dissimilar overall architecture have now been discovered. Most notably different are the overall topologies of interleukin-1β-converting enzyme, a cysteine proteinase which may act as a trigger responsible for cell death (apoptosis) (Walker *et al*., 1994), and 3C-proteinases from picornoviruses. The latter enzymes have a serine protease type overall architecture but with a cysteine instead of a serine residue as an active site nucleophile (Allaire *et al*., 1994; Carrell *et al*., 1994; Matthews *et al.*, 1994).

These conserved catalytic cysteine and histidine ion pairs have pK_a's widely divergent from those of the two amino acids in solution [this type of effect is described by Del Buono *et al.* (1994)]. Although the conserved cysteine ionizes at pH 2.45−3.4, activity does not increase substantially until another active site residue loses a proton at around pH 4.0. In the serine proteinases, this promoter of full catalytic activity is an aspartic acid physically close to the histidine. The equivalent aspartic acid in caricain is at position 158. In the mammalian cysteine proteinases, cathepsins B and H, uncharged glycine and asparagine, respectively, are present at the equivalent position. However, in these cathepsins, there is an arrangement of ionized residues producing a charged environment around the active site ion pair which may be analogous to that given by Asp 158 in caricain. In the proteinase papain when charge was completely removed at 158, there was a considerable reduction in activity (Ménard *et al*., 1991), but surprisingly, D158N gave only a 6-fold decrease in activity, indicating only a limited role for Asp 158. Our work with caricain (EC 3.4.22.30) (Taylor *et al*., 1994), an enzyme structurally very similar to papain, has however indicated a major role for Asp 158 in the catalytic mechanism.

When the enzyme is separated from *Carica papaya*, the profiles produced when k_{cat}/K_M is plotted versus pH cannot be explained solely on the basis of the ionization produced by the ion pair. Other ionizations can be identified by using steady state kinetics and the substrate Pyr-Phe-Leu-*p*NA[1] (Goodenough & Owen, 1987; Sumner *et al.*, 1993). Caricain was cloned and overexpressed (Revell *et al.*, 1993) and the aspartate at position 158 mutated (Taylor *et al.*, 1994). Full catalytic competence was only generated by protonic dis-

[†] N.A.K. acknowledges funding from the Alexander S. Onassis Public Benefit Foundation scholarship (group "O"-115). P.W.G. acknowledges funding from the Institute of Food Research.

* Corresponding author. Telephone: 00 44 1734 316332. Fax: 00 44 1734 753676. E-mail: P.W.Goodenough@Reading.ac.uk.

[⊗] Abstract published in *Advance ACS Abstracts,* November 1, 1996.

S0006-2960(96)00949-X CCC: $12.00

sociations at pH 3.47, 5.23, and 5.57 on the acid side of neutrality (Taylor *et al.*, 1994).

D158N showed no greater activity against the substrate described above than D158A, and we postulate that there is a need for a specific charged environment around the cysteine and histidine in this topology; without this environment, the activity of the Cys-His dyad is inconsequential (Taylor *et al.*, 1994). Supporting evidence for this comes from recalculation of the data of Ménard *et al*. (1991) by Mellor *et al.* (1993b) which indicated that relatively little catalytic competence is produced by the ion pair formation alone (Thomas *et al.*, 1994).

As a working hypothesis, we propose that most of the electrostatic field necessary for full catalytic competence in caricain is produced by the closest charged species but other charged carboxyls provide a considerable portion of the field (we highlighted Glu 35, Glu 50, and Glu 57) (Pickersgill, 1988; Pickersgill *et al.*, 1989; Taylor *et al.*, 1994). This is certainly the case in cathepsin B (G158), where no catalytic activity is generated by a protonic dissociation with a pK_a of 3.4 [generally thought to be ionization of cysteine (Lewis *et al.*, 1976, 1981)] but only when another protonic dissociation with a pK_a of 5−6 occurs (Salih *et al.*, 1987). This dissociation could be from one of many other charged amino acids close to the active site.

Taylor *et al*. (1994) showed no activity was generated in D158E caricain by a protonic dissociation with a pK_a of 3.4 (unlike the wild type), but a protonic dissociation with a pK_a of 4.4−4.9 gives catalytic activity. Is this the ionization of the active site cysteine? We set out to answer this question by using a disulfide inhibitor which releases a chromophore group when reacting with cysteine in the stopped-flow time scale (100 ms to 20 s). These types of probes were designed to measure reactivity differences in active site cysteines from crystallographically identical proteinases such as papain and actinidin. Advocates of their use suggest that such probes are the only way of correctly analyzing the electrostatic field in cysteine proteinases where very specific amino acid residues are changed (Mellor *et al*., 1993a). Therefore, the D158E mutant caricain was used to obtain rapid kinetics measurements over a wide pH range. The tertiary structure was also determined. These data were then compared with steady state kinetics data and the corresponding native structure, respectively. It was shown that ionization of cysteine 25 occurred at pH 3.4 (as in wild type). Additionally, three other ionizations were identified. The protonation of the probe at high pH values was considerably greater in the mutant than in the native enzyme.

MATERIALS AND METHODS

Expression of Recombinant protein. Construction of the caricain expression vector was described earlier (Taylor *et al.*, 1992, 1994). Overday cultures of *Escherichia coli* with the vector carrying the pLysS plasmid were grown in 10 mL of LB broth at 37 °C with ampicillin at 50 μg/mL and chloramphenicol at 25 μg/mL (Taylor *et al.*, 1992). Overnight cultures (500 mL of LB broth inoculated with 1 mL of the overday culture) were used to inoculate 10 L of LB broth. These cells were grown in a 20 L fermenter to an A_{600} of 0.4−1.0 by using 400 rpm impeller agitation, 20 L/min air flow, 3 psi relative pressure, and 37 °C. Induction was by IPTG at a final concentration of 0.1 mM. Samples were removed every 20−40 min and centrifuged in Eppendorf tubes and the cell pellets resuspended in SDS−PAGE gel-loading buffer (Laemmli, 1970). After the solution was heated at 95 °C for 2−5 min, debris was removed by centrifugation and the supernatants were analyzed by SDS−PAGE in 12% gels (Laemmli, 1970). After the solution was heated at 95 °C for 2−5 min, debris was removed by centrifugation and the supernatants were analyzed by SDS−PAGE in 12% gels (Laemmli, 1970).

Cells were harvested 3−4 h postinduction with a Sartorius filtering system and a Watson-Marlow pump. After centrifugation at 5860*g* for 10 min at 4 °C, the cell pellet was suspended in a 50 mM NaH_2PO_4 pH 8.0 buffer containing 50 mM NaCl, 1 mM EDTA, and 0.1 mM PMSF (to inhibit proteolysis). After lysing by passage through a French press (SLM AMINCO, Urbana, IL) at 760−780 psig, insoluble material was collected by centrifugation at 5860*g* for 10 min at 4 °C, washed with pH 8.0 phosphate buffer, and stored at −20 °C (Taylor *et al.*, 1992).

Solubilization and Renaturation. Buffers were degassed and filtered through 2.2 μm Millipore filters. Insoluble material, mainly inclusion body protein, was made soluble by denaturation in 0.1 M Tris-acetate (pH 8.6) containing 6 M guanidine hydrochloride as the chaotropic agent and 10 mM dithiothreitol (as the reducing agent for the thiol groups) at a final concentration of 10 mg/mL and at room temperature for 1 h. After 10-fold dilution by 0.5 M Tris-acetate (pH 8.6) containing 6 M guanidine hydrochloride and 0.1 M oxidized glutathione and incubation at 4 °C for 24 h, the protein was diluted 50-fold into 0.1 M Tris-acetate (pH 8.6) refolding buffer containing 3 mM L-cysteine and 0.4 M L-arginine (Taylor *et al*., 1992, 1994). The refolding buffer was filtered through a 4.5 μm filter due to its viscosity, and to prevent oxidation of the cysteine residues, nitrogen was bubbled through the buffer to remove molecular oxygen. A Pharmacia LKB peristaltic pump transferred the unfolded protein into the 10 L of stirring buffer at a flow rate of 4−6 mL/min. A Verder peristaltic pump was used to recirculate the refolding buffer at a flow rate of about 1 l/min. A tube from the Pharmacia pump was directed through a hole 1.5 in. above the outflow of the Verder tubing. Thus, the recirculating buffer flushed the unfolded protein solution into the buffer at a flow rate 150−250 times greater than the rate of direct dilution. This prevented the development of local high concentrations of protein (Figure 1).

Purification of Refolded Recombinant Protein. Refolded protein was centrifuged at 12000*g* for 10 min at 4 °C and concentrated 50-fold by means of filtration through hollow fibers and finally 10-fold by nitrogen pressure dialysis in an Amicon stirred cell over a YM10 membrane. After desalting through a Sephadex G15 column, using as a buffer 50 mM sodium acetate (pH 5.0) with 0.5 M NaCl, 5 mL fractions which showed activity were slowly diluted 2-fold with 50 mM sodium acetate buffer (pH 5.0). Fractions (1 mL) obtained after loading active samples onto a Mono S HR5/5

[1] Abbreviations: 2 PDS, 2,2′-dipyridyl disulfide; Pyr-Phe-Leu-*p*NA, L-pyroglutamyl-L-phenylalanyl-L-leucine *p*-nitroanilide; PMSF, phenylmethanesulfonyl fluoride; E64, 1-[(L-*trans*-epoxysuccinyl)-L-leucylamino]-4-guanidinobutane [E64 is also called (L-3-*trans*-carboxyoxyran-2-carbonyl)-L-leucylagmatin (Peptide Institute, Osaka, Japan); OMS, organomercurial Sepharose; DMSO, dimethyl sulfoxide; DTNB, 5,5′-dithiobis(2-nitrobenzoic acid); RMS, root mean square; CCP4, Collaborative Computational Project 4, Daresbury, England; IPTG, isopropyl β-D-thiogalactopyranoside.

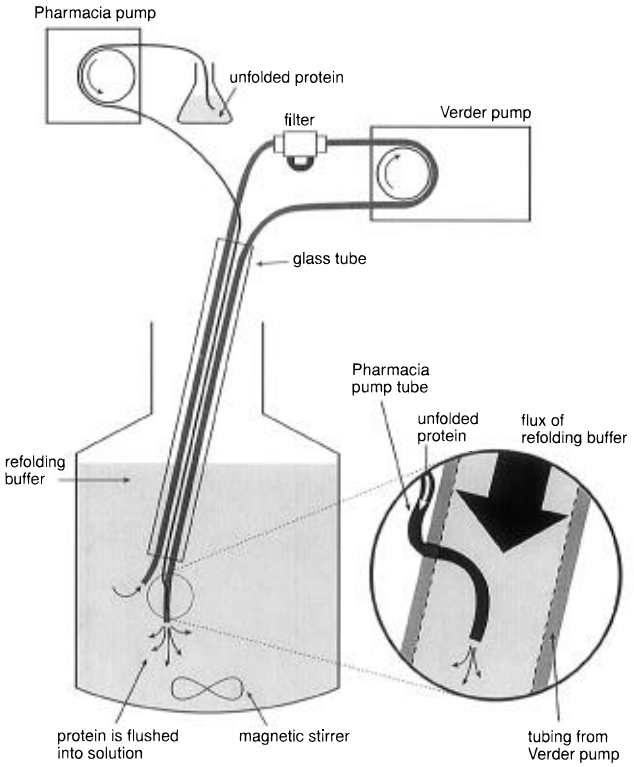

FIGURE 1: Experimental setup for refolding buffer recirculation and elimination of diffusion as a controlling step in the refolding process.

column and eluting with a gradient of 0 to 1 M NaCl containing 2 mM $HgCl_2$ in 50 mM sodium acetate buffer (pH 5.0), were then stored at 4 °C (Taylor *et al*., 1992, 1994).

Blots. Gradient 10 to 27% Tris-glycine gels (Novex Corp.) were used to identify protein constituents of different Mono S peak fractions. Excess E64 prevented autolysis when incubating with reducing agent at 95 °C prior to adding sample to the gels. Protein was transferred to Millipore Immobilon PVDF transfer membranes by using carbonate sample buffer (pH 9.9) containing 20% MeOH (Dunn, 1986). Ponceau S was used to stain the proteins on the membrane. The N-terminal sequence of those proteins of interest was determined.

Activation Assays. Enzyme activity was determined by the release of *p*-nitroaniline from Pyr-Phe-Leu-*p*NA at 37 °C and pH 7.0 in flat-bottomed ELISA plates.

Either an Anthos 2000 Labtec plate reader at 405 nm or a double-beam Perkin-Elmer Lambda 15 spectrophotometer was used to monitor *p*-nitroaniline release (Taylor *et al*., 1992, 1994).

Selection of Active Sites Using an Organomercurial Sepharose Column. OMS columns (5 mL of Sephadex G-15) were used for selection of active enzyme molecules with reduced thiol groups in the active site (Sluyterman & Wijdenes, 1970). Three buffer solutions were prepared for the selection process: (1) regenerating buffer, 50 mM sodium acetate (pH 4.8) containing 10 mM $HgCl_2$ and 20 mM EDTA (buffer A); (2) 50 mM sodium acetate wash buffer (pH 5.5) with 1 mM EDTA and 200 mM NaCl (buffer B); and (3) cysteine buffer with the same constituents as buffer B with freshly added 10 mM cysteine (buffer C).

Fractions were activated through addition of excess free cysteine (final concentration of 10 mM) and 4 mM EDTA. Activated enzyme was then desalted by passing through a G-15 column with buffer B so that excess free cysteine and chelated mercury ions were removed. After being washed with buffer B, the OMS column was used to separate oxidized forms of the enzyme from reduced forms. Oxidized enzyme would not bind to the affinity matrix of the OMS, whereas the reduced form of the enzyme was bound and then eluted with buffer C. These 2 mL fractions were desalted with a 0.1 M KCl and 1 mM EDTA solution (Mellor *et al*., 1993b). The OMS column was regenerated with buffer A and stored.

E64 Titration. In order to measure the concentration of available active sites in a cysteine protease like caricain, it is necessary to combine use of active site-directed irreversible inhibitors (which do not necessarily release chromophoric groups upon binding with the enzyme) and a sensitive catalytic assay (like the one described in the above section). One such inhibitor which binds irreversibly and very specifically at a 1:1 molecular ratio with the active site of most cysteine proteinases is E64 which is extracted from cultures of *Aspergillus japonicus* (Hanada *et al*., 1978).

Titration of cysteine protease solutions with E64 involved preparing serial dilutions of 10 mM E64 solution in DMSO by using a phosphate assay buffer [0.2 M NaH_2PO_4 (pH 7.0) containing 10 mM L-cysteine, 1 mM EDTA, and 0.05% Brij]. Aliquots (5−10 μL) of enzyme solutions were mixed with equal volumes of E64 dilutions in flat-bottomed ELISA plates and left to incubate at room temperature for 10 min. One hundred microliters of 0.3 mM Pyr-Phe-Leu-*p*NA in assay buffer was added to each well of inhibited enzyme and the release of *p*-nitroaniline measured in the plate reader at 405 nm to estimate the activity of the noninhibited enzyme. The intercept of the plot of absorbance readings A_{405} versus E64 concentration with the ordinate axis gave the concentration of enzyme active sites.

Ellmann's Assay. After L-cysteine had been used to activate the proteinase, it had to be removed completely to prevent its reaction with the thiol specific probes. Ellmann's assay is a sensitive technique to detect low-molecular weight thiols such as cysteine (free thiols).

A solution of 3 mM DTNB (Ellmann's reagent) in 0.1 M phosphate (pH 7.27) with 1 mM EDTA was prepared. Two aliquots of 3 mL of buffer were equilibrated in plastic cuvettes in the thermostated sample and reference compartments of the spectrophotometer, and the A_{412} was adjusted to 0. A 100 μL aliquot of stock buffer was added to the reference cuvette, and the solution was stirred with a flat-ended glass stirring rod. DTNB solution (100 μL) was added to the sample cuvette with stirring, and the A_{412} of the DTNB was recorded (A_{DTNB}). The cysteine-free solution (100 μL), which had been used for dialysis or elution of the protein, was added to the reference cuvette with stirring and, finally, 100 μL of the protein diffusate or eluate added to the sample cuvette with mixing, and the A_{412} was recorded until the reaction was complete (A_{final}) (Riddles *et al*., 1983). To be able to accept a protein solution for stopped-flow measurements using thiol specific time dependent inhibitors as reactivity probes, the difference in absorbance readings was $A_{final} - A_{DNTB}$, <0.001 absorbance unit.

Stopped-Flow Rapid Kinetics Experiments. Reaction of 2 PDS with both wild type and mutant caricain was used as the basis for analysis of fast reaction kinetics. A stopped-flow spectrofluorimeter (Hi-Tech Scientific) was used with a kinetics workstation and data acquisition and analysis

software. Reactions occurred at 25 °C and at a constant ionic strength of 0.1 M in solutions containing 1 mM EDTA under pseudo-first order conditions where [disulfide] ≫ [caricain D158E]. Monochromator entrance and exit slit widths were set at 1 mm, and the absorbance change (due to release of the chromophore group 2-mercaptopyridine) was measured at 343 nm (Mellor *et al.*, 1993b; Topham *et al.*, 1991). The concentration of enzyme in the mixing chamber was 3−5 μM, and that of the probe was 150 μM. Buffers were in the pH range 2.01−10.20 at steps of 0.05−0.15 [as described by Salih *et al.* (1987)]. The pH meter was calibrated between pH's 2 and 3, 3 and 4, 4 and 5, 5 and 6, 6 and 7, and 7 and 10 (±0.02) with standard solutions before making the particular buffer. Data were collected using a time constant of 33 ms, with oversampling. A 1 MHz analog-to-digital converter of a 286 Epson personal computer was interfaced with the stopped-flow machine. To obtain the first-order rate constants k_{obs}, two models were used to fit the acquired absorbance versus time ($A-t$) data. The first was a single exponential with an offset, i.e.

$$A(t) = P_1 \exp(-P_2 t) + P_3$$

where $P_1 = A_0 - A_{inf} < 0$ (A_0 and A_{inf} are the initial and final absorbances measured in a set time in the sample-handling unit of the stopped-flow machine), $P_2 = k_{obs}$ (s^{-1}), and $P_3 = A_{inf}$. The second was a single exponential with a first-order (with respect to time) component and an offset, i.e.

$$A(t) = P_1 \exp(-P_2 t) + P_3 t + P_4$$

where $P_1 = A_0 - A_{inf}$, $P_2 = k_{obs}$ (s^{-1}), P_3 = the slope of the first-order component (s^{-1}), and P_4 = the extrapolated value of the ordinate intercept which in the case of the first model is equal to A_{inf} (Mellor *et al.*, 1993b). The linear relationship between k_{obs} and disulfide concentration at pH 4.6 and 8 was verified ([enzyme] = 3−5 μM and [disulfide] = 60, 80, 100, 150, and 300 μM). The second-order rate constant k was then calculated from $k = k_{obs}$/[disulfide]. The statistical package BMDP was used to fit multiple ionization models to the k_{obs} values. Initial estimates were obtained by inspection and program 3R (nonlinear regression) used to obtain the best fit. The RMS deviation between observed and calculated observations is given in the results. The number of observations was 179.

Crystallization. Crystals were produced using hanging drop methods. Purified fractions were checked for the correct N-terminal sequence, and activity was inhibited with E64. The final protein concentration was 13 mg/mL, and 3 μL of this was mixed with 3 μL of 0.3 M $(NH_4)_2SO_4$ and 29% PEG 1000 at 18 °C.

Collection of Synchrotron Data and Processing. Data were collected from a single crystal of the D158E mutant caricain/E64 complex using synchrotron radiation from beam line BL-6A2 at the Photon Factory, KEK, Tsukuba, Japan (Sakabe *et al.*, 1995). A Weissenberg geometry was used in the collection device, with a cassette radius of 429.7 mm with two 20 × 40 cm image plates placed horizontally one above the other. The coupling constant was 1.5 deg/mm, and each exposure consisted of 30 repeats of a 10.5° oscillation range at a rate of 2 deg/s with 0.5° overlap with the preceding range. The total oscillation range covered was 180.5°, corresponding to 36 image plates. Crystal orientation and crystal parameters were determined from 1.0° oscillation photographs; data were reduced using the program DENZO (Otwinowski, 1993) on a Silicon Graphics Indigo^2 extreme workstation, and programs from the CCP4 suite were used for the final internal scaling and merging of the data.

Molecular Replacement and Refinement. Rotation and translation functions were solved using the X-PLOR program package (Brünger *et al*., 1987). Native caricain coordinates (ignoring the bound mercury coordinates) (Pickersgill *et al*., 1991) were used as the search model, and the range of data used in the rotation function was 15.0 through 4.0 Å. An Evans and Sutherland PS390 graphics system running program FRODO (Jones, 1978) was used to fit E64 into the electron density area of the map, and a glutamate side chain was substituted for aspartate at position 158. A topology and a parameter file for E64 was introduced into X-PLOR for the later stages of refinement. A cross-validation criterion was provided by 50 cycles of the automated refinement procedure (Lamzin & Wilson, 1993) run in restrained mode with protein and water coordinates only. Another means of cross-validation involved simulated annealing using X-PLOR. This used protein coordinates only with position 158 mutated into a Gly in order to ensure that the position of the E64 and of the glutamate 158 side chain were not over-refined in the proposed model. Water molecules were included in the final model with the criterion of having good density at 1 RMS contour level in the $2F_{obs} - F_{calc}$ map. The model used in the final X-PLOR positional and *B*-factor refinement contained caricain with the glutamate at position 158. E64, 94 water molecules, and an ethanol molecule were fitted in the electron density of the $2F_{obs} - F_{calc}$ map. The program PROCHECK (Laskowski *et al*., 1994) was run on the final model as a cross-validation criterion of over-refinement. The final coordinates of the structure, as well as the structure factors, have been submitted to The Protein Data Bank (identification codes 1MEG and R1MEGSF, respectively).

RESULTS

Refolding and Purification of Recombinant Protein. A novel refolding procedure was used which made it unnecessary to activate denatured enzyme by incubating at pH 4.0 for 10 min at 60 °C (Taylor *et al*., 1994). Figure 2 illustrates that incubation at pH 8.6 during the refolding process gave a mixture of enzyme with and without the pro region. These two forms could be separated by ion exchange chromatography.

If refolded directly after fermentation, the protein was unprocessed enzyme. However, after that was frozen for 2 or 4 weeks, a mixture of processed and unprocessed enzyme was present, indicating that processing to active enzyme occurs during aging.

If the enzyme was left to recirculate by reversing the direction of flow through the hollow fibers for 1−2 h at room temperature, activation and processing were enhanced. Protein fractions from the ion exchange chromatography were "Western blotted" and used for N-terminal sequencing. Only the processed material which had Leu-Pro-Glu-Asn as the N-terminal sequence (Dubois *et al.*, 1988) was used for crystallization.

Reactions with 2 PDS. Very good resolution of the experimental curves for even small pH changes was obtained,

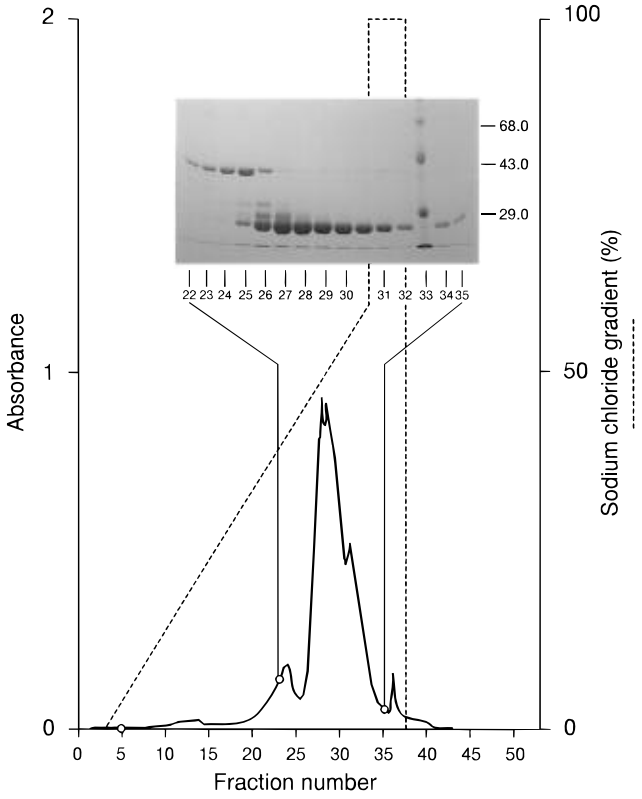

FIGURE 2: Mono S eluent after refolding of the insoluble pellet. This shows two peaks which can be differentiated by 12% SDS−PAGE gels into processed and unprocessed fractons. This indicates that processing takes place during the refolding operation without having to incubate the enzyme at 60 °C for 10 min at pH 4.0.

and also good was the sensitivity in the range of 10 milliabsorbance units. The reaction between 2 PDS and wild type caricain was monitored between pH 2 and 10 at single pH intervals. The data confirmed the published results for that reaction (Topham *et al.*, 1991) and validated the method for use with the mutants.

The general formula used to determine reaction rate k is given in eq 1. A_i is a generalized pH independent constant

$$k = \sum_{i=1}^{n} \frac{A_i}{(1 + \sum_{j=1}^{n} B_{ij})} \quad (1)$$

corresponding to each protonic state i. The denominator accounts for the contribution of each protonic state i to the overall reaction rate k with varying pH. The B_{ij} terms are products of macroscopic dissociation constants K and/or their reciprocals ($1/K$) and powers of proton concentration (H^+) according to information matrices 1 and 2 described in Topham *et al*. (1991). Using the statistical package BMDP, both a six-parameter model (three pK_a's and three independent rate constants) and an eight-parameter model (four independent rate constants and four pK_a's) were fitted to the data. The residual mean squares were 0.0357 and 0.0168 for the six- and eight-parameter models, respectively. The six-parameter model had 173 degrees of freedom, and the eight-parameter model had 171 degrees of freedom. Addition of further parameters did not improve the fit of the data. The equation for the eight-parameter model is shown below, and the fit of the equation to the data is shown in Figure 3.

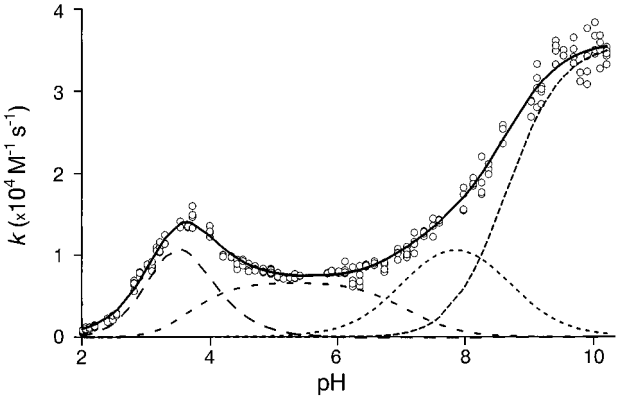

FIGURE 3: Stopped-flow results of the second-order rate constant k versus pH for the reaction of Asp158Glu mutant caricain with 2 PDS plotted together with the theoretical line which corresponds to a model comprising four pH independent rate constants and four pK_a's. The four components of the model are also depicted on the plot.

$$k = \tilde{k}_1/[1 + [H^+]/K_1 + K_2/[H^+] + K_2K_3/[H^+]^2 + K_2K_3K_4/[H^+]^3] + \tilde{k}_2/[1 + [H^+]^2/(K_1K_2) + [H^+]/K_2 + K_3/[H^+] + K_3K_4/[H^+]^2] + \tilde{k}_3/[1 + [H^+]^3/(K_1K_2K_3) + [H^+]^2/(K_2K_3) + [H^+]/K_3 + K_4/[H^+]] + \tilde{k}_4/[1 + [H^+]^4/(K_1K_2K_3K_4) + [H^+]^3/(K_2K_3K_4) + [H^+]^2/(K_3K_4) + [H^+]/K_4] \quad (2)$$

The fitted values for k, taking into account that the pK_a of the probe was 2.45, were as follows: $\tilde{k}_1 = (2.93 \pm 0.080) \times 10^4$ M^{-1} s^{-1}, $\tilde{k}_2 = (0.68 \pm 0.020) \times 10^4$ M^{-1} s^{-1}, $\tilde{k}_3 = (1.41 \pm 0.120) \times 10^4$ M^{-1} s^{-1}, and $\tilde{k}_4 = (3.58 \pm 0.027) \times 10^4$ M^{-1} s^{-1}; p$K_1 = 3.42 \pm 0.03$, p$K_2 = 3.57 \pm 0.04$, p$K_3 = 7.08 \pm 0.15$, and p$K_4 = 8.64 \pm 0.06$.

Crystallization. Crystals used for diffraction experiments were small needles with the dimensions 0.15 mm × 0.05 mm × 0.05 mm. The unit cell dimensions were as follows: $a = 53.45$ Å, $b = 65.33$ Å, $c = 64.37$ Å, and $\beta = 111.60°$ ($C2$ monoclinic space group); there was one molecule per asymmetric unit.

Data Processing and Refinement. Using X-PLOR, the rotation function solution (202.8, 85.0, 265.8) was at a peak height of 5.1 times the RMS value above the next highest peak and 7.7 times the RMS value above the mean. The translation function solution (−0.7, 0.0, 22.4) was 6.9 times the RMS value above the next highest peak and 8.9 times the RMS value above the mean. The reliability index (R factor) was then reduced from 0.462 to 0.387 by rigid body refinement using data in the range 10.0 through 2.0 Å. The first unbiased proof that E64 was bound to the active site cysteine was the $2F_{obs} - F_{calc}$ map that was calculated from the rigid body refined molecular replacement solution in which there was an area of electron density clearly visible in the active site. Further use of X-PLOR for positional and temperature factor refinement, including waters and E64, reduced the R factor for protein, water, and E64 to 0.211. After the final correction to the E64 conformation selection of the water molecules that displayed good electron density only, and the final positional and B-factor refinement in X-PLOR, the R factor dropped to 19.3.

The next step in structural validation (ARP in restrained mode) reduced the R factor from 0.202 to 0.153. In the

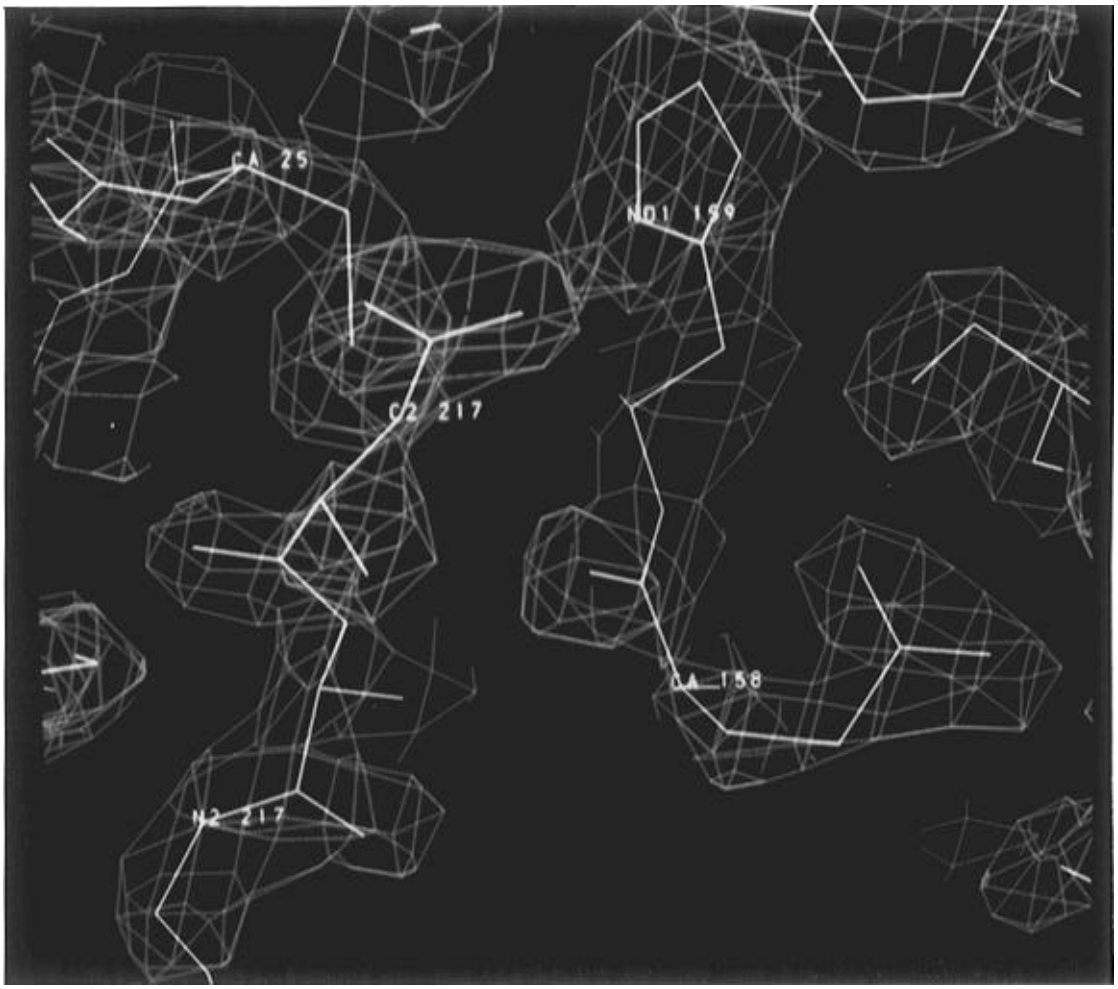

FIGURE 4: Simulated omit map calculated for D158E caricain proving that there is a glutamate at position 158.

resulting $3F_{obs} - 2F_{calc}$ map, water molecules had been fitted by the program in the E64 area of electron density mimicking the shape of the inhibitor, and this was another unbiased piece of evidence proving the correct position of E64 in the model. Finally, a simulated annealing routine in the program X-PLOR gave density corresponding to E64. Thus, electron density for E64 and the side chain at position 158 were clearly visible in the calculated simulated annealed omit map. This proved that the side chain was a glutamate as shown in Figure 4 and that it was correctly positioned in the model.

Structure of the D158E/E64 Caricain Complex. The final model has an *R* factor of 0.193 and acceptable stereochemistry according to the Ramachandran plot (see Figure 8) and the statistics produced by PROCHECK.

The final calculated $2F_{obs} - F_{calc}$ map shows that the position of side chain Glu 158 in mutant caricain is similar to that of Asp 158 in the wild type and bears a similar conformation. There is a similar hydrogen-bonding network between residues Ser 136 and Lys 137 and both the carboxy moiety of Asp 158 in the native enzyme and Glu 158 in the mutant. A comparison of the hydrogen-bonding networks can be seen in Table 1 and Figure 6.

In the mutant, the carboxyl oxygen OE2 of Glu 158 is closer to Ser 136 and Lys 137 than that of Asp 158 in the wild type. Generally, when the carboxyl oxygens of the mutant are orientated toward His 159, the distances remain the same. Ménard *et al.* (1991), in papain, showed a hydrogen bond between the carboxyl oxygen of Asp 158

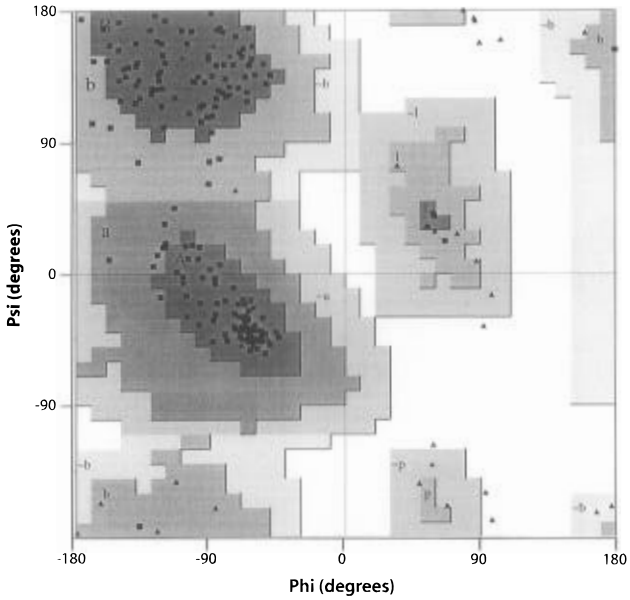

FIGURE 5: Ramachandran plot of the final protein model displayed by PROCHECK and proving the stereochemical correctness of the structure. Residues in the most favored regions (A, B, and L) number 150 (88.2%). Residues in additionally favored regions (a, b, l, and p) number 20 (11.8%).

and the main chain nitrogen of His 159, and there is a similar distance between these residues in caricain. We consider the hydrogen bond to be too weak to be significant. The final $2F_{obs} - F_{calc}$ map shows a covalent link between the

Table 1: Hydrogen Bonds Involving the Side Chain of Amino Acid 158

hydrogen bond	caricain (D158)	D158E caricain/E64 (E158)
OD2(OE1)−NZ(137)	2.82	2.98
OD2(OE1)−N(137)	3.10	2.74
OD1(OE2)−N(136)	2.74	2.91
OD1(OE2)−OG(136)	2.73	2.83

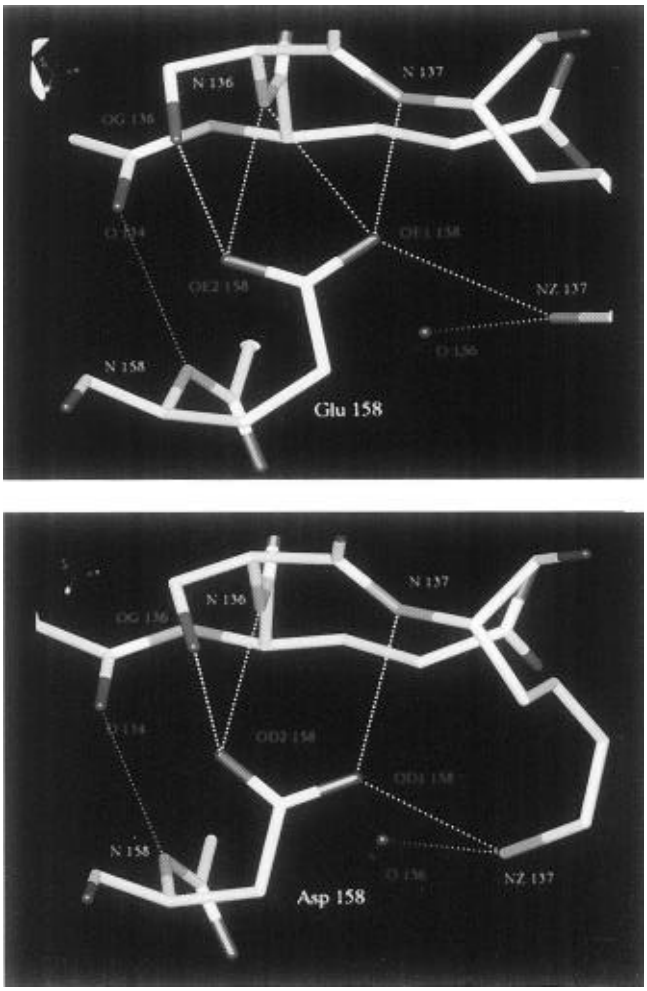

FIGURE 6: Comparison of the hydrogen-bonding pattern between the Glu 158 side chain in D158E mutant caricain (top) and native caricain (bottom). A hydrogen-bonding distance cutoff of 3.2 Å was used because we think this distance will still give a strong hydrogen bond. However, Ménard *et al.* (1991) have a greater cutoff distance, and this allows them to show a long hydrogen bond from the carboxyl oxygen of Asp 158 to the main chain nitrogen of His 159. We do not show this bond in this figure because we consider it too weak to be significant.

C2 atom of E64 and the SG atom of cysteine 25 as well as the interaction of the leucyl moiety with the S2 subsite in the active site, as described by Drenth *et al*. (1968) and Schechter and Berger (1967). What is quite striking, however, is that the 4-guanidinobutane moiety is not visible in the electron density map in the D158E caricain structure, and the last atom within electron density is the carbon atom following N2. A more detailed comparison of hydrogen-bonding distances made by E64 and active site residues in D158E caricain/E64, papain/E64 (Varughese *et al*., 1989), and actinidin/E64 (Varughese *et al*., 1992) complexes is presented in Table 2 and Figure 7 (top, middle, and bottom).

Table 2: Comparison of Hydrogen Bonds Between E64 and D158E Caricain with Similar Patterns in Papain and Actinidin

E64	caricain	papain	actinidin	distances (Å)		
O1	ND1(159)	ND1(159)	ND1(162)	2.89	2.90	2.75
O1	O(H_2O 310)	O(H_2O 217)	O(H_2O 582)	2.98	2.67	2.73
O2	NE2 (19)	NE2 (19)	NE2 (19)	2.74	2.87	2.86
O2	N(24)	N(24)	N(24)	3.32	3.11	3.33
O2	N(25)	N(25)	N(25)	3.01	2.95	2.89
O3	no contact	no contact	O(H_2O 586)	–	–	2.65
O4	N(66)	N(66)	N(68)	2.79	2.88	2.90
N1	O(158)	O(158)	O(161)	3.27	3.40	3.10
N2	O(66)	O(66)	O(68)	2.94	3.04	2.87
N3	not visible	no contact	O(H_2O 54)	–	–	2.97
N4	not visible	OH (61)	O(H_2O 54)	–	2.96	3.49
N4	not visible	O(H_2O 216)	O(H_2O 257)	–	2.45	3.43
N5	not visible	OH (67)	O(66)	–	2.93	3.35

Another very important feature of this structure is its slight expansion in comparison with the native structure (Pickersgill *et al*., 1991). This expansion is shown in the overall structure as a subtle opening of the active site cleft which incorporates the E64 inhibitor. At a local level, it can be identified between the part of the main chain which carries the Glu 158 side chain and the part carrying Ser 136 and Lys 137; these interact by hydrogen bonding with the carboxyl group of Glu 158.

The source of the ethanol molecule that has been fitted in the elongated region of electron density is probably ethanol that had been used as a solvent for E64 when making the crystals (see Materials and Methods).

DISCUSSION

Refolding and Activation of pro-Caricain. Previous studies by the groups of Ménard (Vernet *et al*., 1989, 1990) and Goodenough (Taylor *et al*., 1992) have used refolding protocols which include an activation step. This step involved treating the proenzyme at 60 °C and pH 4.0 to autocatalytically remove the 107 amino acids of the proregion. In this work, a modified refolding method separated the proregion and activated the enzyme by treatment at pH 8.6 and either 4 or 25 °C. This new regime is less harmful to the enzyme. More processed enzyme was obtained after storage as frozen insoluble inclusion bodies than from material used immediately after harvest. The proregion thus appears quite labile and is easily cleaved form the mature enzyme. The N-terminal amino acid of the mature protein is leucine (correct N terminus), but sometimes up to four amino acids of the proregion remained attached. This phenomenon has been reported by Vernet *et al.* (1990) and Taylor *et al.* (1992, 1995), and only correctly processed enzyme was used for crystallography. Enzyme protein with the four extra amino acids was found to have the same activity as wild type.

Structural Data. There is no native caricain/E64 complex structure available, and the other available structures of complexes with this inhibitor, namely actinidin/E64 and papain/E64, either show clear electron density for the entire E64 molecule in the former case (Varughese *et al*., 1989) or have difficulty locating it entirely in the latter case (Varughese *et al*., 1992). The hydrogen-bonding comparison between the D158E caricain/E64, papain/E64, and actinidin/E64 complexes shows that the hydrogen-bonding network is similar in the three cases. However, the equivalent bonding to that between His 61 and Tyr 67 in caricain is

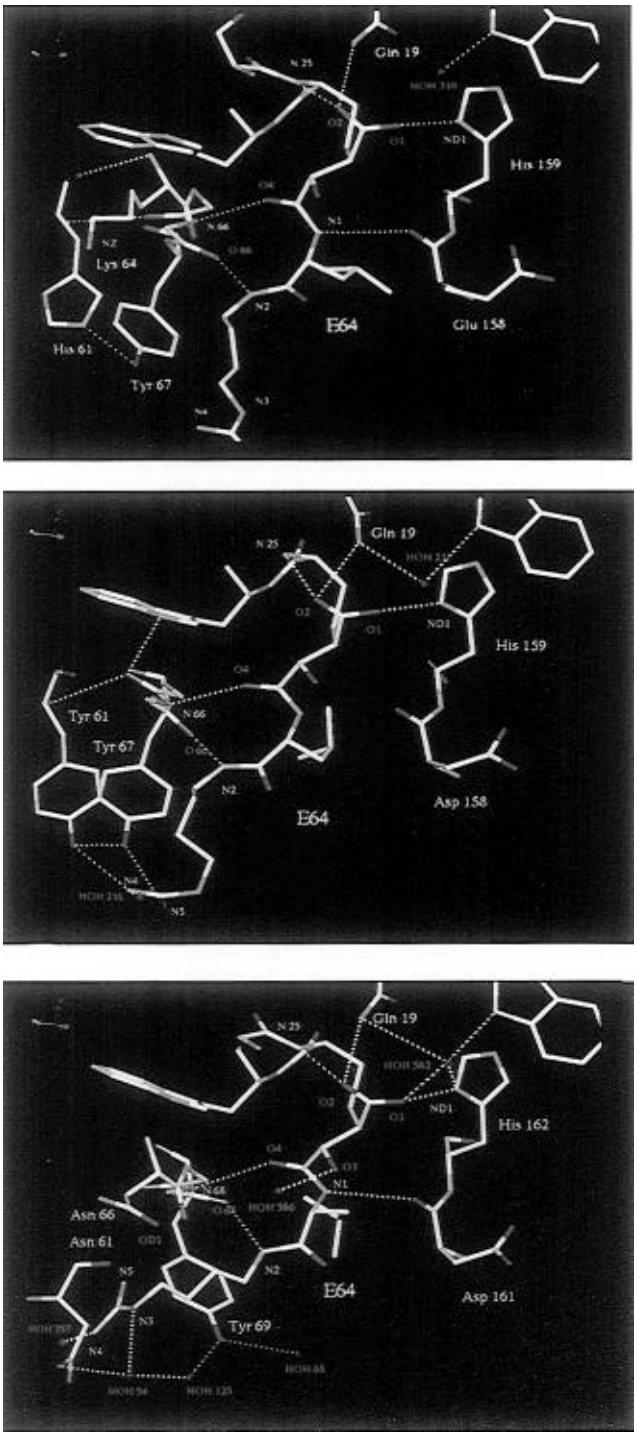

FIGURE 7: Hydrogen-bonding comparison of E64 in the active sites of (top) D158E caricain, (middle) papain, and (bottom) actinidin in corresponding structures of the complexes.

between Tyr 61 and Tyr 67 in papain. In actinidin, the hydrogen-bonding effect of these two pairs of residues is replaced by Asn 61, Asn 66, and Tyr 69, together with a very well-ordered hydrogen-bonded network of water molecules of which the most important are 54 and 125. In the papain active site, hydrogen bonds between the N4 atom of E64 and the OH of Tyr 61 and between N5 and the OH of Tyr 67 hold the guanidinium moiety of E64 tightly enough to make it seen in density. On the other hand, in caricain, residue 61 is a histidine and its NE2 atom interacts with the OH of Tyr 67, so there are no hydrogen bonds made with any of the nitrogen atoms of the 4-guanidinobutane moiety

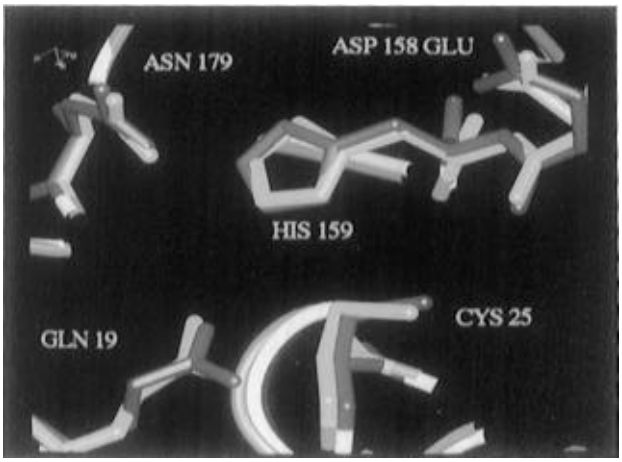

FIGURE 8: Comparison of the conformations of key residues in the active site. The changes are all very subtle except for position 158 where the carboxy moiety of the Glu 158 is orientated more toward His 159 than the carboxy moiety in Asp 158 in the native caricain. Yellow is native caricain, and red is D158E.

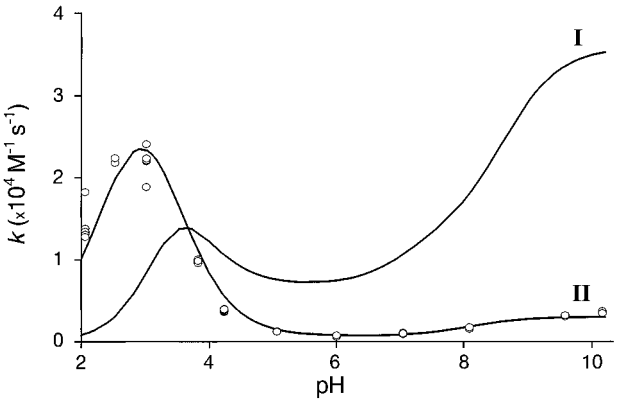

FIGURE 9: Comparison of the stopped-flow results acquired in this work for D158E mutant caricain (curve I) and for native caricain (curve II) showing good reproducibility of the published results (Topham *et al.*, 1991) for the fitted pK_a's but slightly higher second-order reactivity rates.

of E64. Thus, this moiety can move freely and is not visible in electron density. E64 does not interfere with the positioning of the Glu 158 side chain since it does not interact via any hydrogen bond with it.

Structural Data for the Glu 158 Side Chain. The structural data for the mutant indicate that the overall size of the active site is the same as in the wild type. However, the main difference is a different orientation of the oxygens from Glu 158 to the imidazolium ion. There is a similar hydrogen-bonding pattern between Glu 158 in D158E caricain/E64 and Asp 158 in native caricain. Although the distances between the His 159 ND1 atom and the carboxyl oxygens only change from 5.52 Å for OD1 and 7.40 Å for OD2 (Asp 158) to 5.53 Å for OE1 and 7.56 Å for OE2 (Glu 158), there is rearrangement of the histidine-glutamate configuration (Figure 8).

Because of the minute change in these distances, we are led to the conclusion that the protonation enhancement of the probe is stereochemically related and is probably due to the new conformation of the Glu 158 side chain.

Rapid Kinetics Results. The data summarized in Figure 9 comprise the first report which compares the reaction of 2 PDS with the active site cysteine from both wild type and mutant proteinases. Protein crystallography was used to

clearly show the structural differences between native and mutant enzyme.

The profiles of the second-order kinetic constant *k* versus pH are remarkably different from those of native and mutant enzymes. However, it must be stressed that no uncombined low-molecular weight "free" thiols were present in solution, thereby ruling out artifactual results (Figure 9).

The probe used was chosen for its fundamental properties, i.e. that different reactivities exist for each of the two protonic or ionization states (Brocklehurst & Little, 1973) and that 2 PDS increases its electrophilicity by 1000-fold on protonation of the ring N or by contact with a hydrogen-bonding donor (Brocklehurst, 1982; Brocklehurst *et al*., 1987, 1988). In native cysteine proteinase/reagent complexes, such a hydrogen-bonded contact is not made, producing the pH−*k* profile shown in Figure 9 for the wild type caricain, with a maximum reactivity at pH 3.0 [discussed in Topham *et al.* (1991)]. In comparison, reaction of the simplest minimal cysteine proteinase catalytic site model (benzimidazol-2-ylmethanethiol) with 2 PDS shows a pH−*k* profile with a maximum at pH 7−8. Plou *et al*. (1996), working with thiosubtilisin and 2 PDS, obtained results similar to those shown for the mutant in Figure 9. D158E has a clear ionization at pH 3.4 (Figure 3). This is the ionization of the cysteine−imidazolium ion pair, (Cys)-SH/(His)-Im^+H ↔ (Cys)-S^-/(His)-Im^+H. Steady state data identify pK_a's of 4.9, 5.1, and 5.87 for D158E. Thus catalytic activity does not develop on ionization of the cysteine but only increases when other ionizations occur (characterized as a pK_a of 3.6 in Figure 3). Fast reaction kinetic data clearly show that there is a big increase in the second-order rate constants of the mutant caricain in the alkaline limb compared with those from the native enzyme. The mutant pK_a value of 8.6 corresponds to the deprotonation of the ion pair, (Cys)-S^-/(His)-Im^+H ↔ (Cys)-S^-/(His)-Im. Thus, it appears that the pyridyl ring is being protonated at high pH. Maybe the active site imidazolium is destabilized at high pH and is thus a more effective hydrogen-bonding donor and protonation reagent in the mutant enzyme.

An alternative possibility, that both His 159 and the acid at 158 are protonating the probe at high pH, was suggested by Shipton and Brocklehurst (1978; see Scheme 3d on p 386). This seems extremely unlikely from our structural data because there is a well-established hydrogen-bonding network between the glutamate side chain in the mutant with three neighboring residues (Figure 6 and Table 2). The apparent enhancement of the ability of histidine 159 to act as a proton donor at high pH in the mutant may be due to the carboxyl of Glu 158 being reoriented relative to the His and thus destabilizing the interaction between Cys 25 and His 159.

In the conditions found in the mutant, the "degree of ionization" (Dixon, 1992) of the active site thiol of Cys 25 is less and another ionization is an absolute requirement for activity. This change in degree of ionization is related to the higher pK_a of a glutamic acid R group when compared to that of an aspartate and also to the subtle change in position of the R group (Tipton & Dixon, 1983).

In conclusion, it seems that there is no change in the pK_a of ionization of the active site cysteine in the mutant; this remains at 3.4 as in the wild type. Therefore, the steady state data indicating an initial ionization at 4.93 in fact represent a combination of more than one ionization. It appears that the cysteine ionization alone is insufficient to support catalysis in the mutant, thus supporting the predictions in Taylor *et al.* (1994) and Mellor *et al.* (1993b). Kinetically influential ionizations in the acid region probably include the acid at position 158 as well as other charged residues. We have highlighted the likely involvement of Glu 50, and further mutational experiments on this residue will help resolve this intriguing system further.

ACKNOWLEDGMENT

The authors thank Dr. Victor Lamzin for providing the latest version of ARP and for useful advice and ex-colleagues at the BBSRC Institute of Food Research for useful discussion.

REFERENCES

Allaire, M., & James, M. N. G. (1994) *Nat. Struct. Biol. 1*, 505−506.
Baker, E. N., & Dodson, E. J. (1980) *Acta Crystallogr., Sect. A: Cryst. Phys., Diffr., Theor. Gen. Crystallogr. 3b*, 559−572.
Brocklehurst, K. (1982) *Methods Enzymol, 87C*, 427−469.
Brocklehurst, K., & Little, G. (1973) *Biochem. J. 133*, 67−80.
Brocklehurst, K., Willenbrock, F., & Salih, E. (1987) in *Hydrolytic Enzymes* (Neuberger, A., & Brocklehurst, K., Eds.) pp 39−158, Elsevier, Amsterdam.
Brocklehurst, K., Brocklehurst, S. M., Kowlessur, D., O'Driscoll, M., Patel, G., Salih, E., Templeton, W., Thomas, E., Topham, C. M., & Willenbrock, F. (1988) *Biochem. J. 256*, 543−558.
Brünger, A. T., Kurysian, J., & Karplus, M. (1987) *Science 235*, 458−460.
Carrell, R. W., & Lesk, A. M. (1994) *Nat. Struct. Biol. 1*, 492−494.
Collaborative Computational Project, Number 4 (1994) *Acta Crystallogr. Sect. D: Biol. Crystallogr. 50*, 760−763.
Del Buono, G. S., Figueirido, F. E., & Levy, R. M. (1994) *Proteins 20*, 85−97.
Dixon, H. B. F. (1992) *Essays Biochem. 27*, 161−176.
Drenth, J., Jansonius, J. N., Koekoek, R., Swen, H. M., & Wolthers, B. G. (1968) *Nature 218*, 929−932.
Dubois, T., Kleinschmidt, T., Schneck, A. G., Looze, Y., & Braunitzer, G. (1988) *Biol. Chem. Hoppe-Seyler 369*, 741−754.
Dunn, S. D. (1986) *Anal. Chem. 58*, 144−153.
Goodenough, P. W., & Owen, J. (1987) *Phytochemistry 26*, 75−79.
Hanada, K., Tamai, M., Yamagishi, M., Ohmura, S., Sawada, J., & Tanaka, I. (1978) *Agric. Biol. Chem. 42*, 523−538.
Heinmann, U. P., Pal, G. P., Hilgenfield, R., & Saenger, W. (1982) *J. Mol. Biol. 161*, 591−606.
Jones, T. A. (1978) *J. Appl. Crystallogr. 1*, 262−272.
Knowles, J. R. (1976) *CRC Crit. Rev. Biochem. 4*, 165−173.
Laemmli, U. K. (1970) *Nature 227*, 680−685.
Lamzin, V. S., & Wilson, K. S. (1993) *Acta Crystallogr., Sect. D: Biol. Crystallogr. 49*, 129−147.
Laskowski, V. S., MacArthur, M. W., & Thornton, J. M. (1994) in *From First Map to Final Model* (Bailey, S., Hubbard, R., & Waller, D. A., Eds.), pp 149−159, Daresbury Laboratory, Daresbury, U.K.
Lewis, S. D., Johnson, F. A., & Shafer, J. A. (1976) *Biochemistry 15*, 5009−5017.
Lewis, S. D., Johnson, F. A., & Shafer, J. A. (1981) *Biochemistry 20*, 48−51.
Matthews, D. A., Smith, W. W., Ferre, R. A., Condon, B., Budahazi, G., Sisson, W., Villafranca, J. E., Jansen, C. A., McElroy, H. E., Gribskov, C. L., & Worland, S. (1994) *Cell 77*, 761−777.
McGrath, E. M., Eakin, A. E., Engel, J. C., McKerrow, J. H., Craik, C. S., & Fletterick, R. J. (1995) *J. Mol. Biol. 247*, 251−259.
Mellor, G. W., Thomas, E. W., Topham, C. M., & Brocklehurst, K. (1993a) *Biochem. J. 290*, 289−296.
Mellor, G. W., Patel, M., Thomas, E. W., & Brocklehurst, K. (1993b) *Biochem. J. 294*, 201−210.

Ménard, R., Khouri, H. E., Plouffe, C., Laflamme, P., Dupras, R., Vernet, T., Tessier, D. C., Thomas, D. Y., & Storer, A. C. (1991) *Biochemistry 30*, 5531−5538.
Musil, D., Zucic, D., Turk, D., Engh, R. A., Mayr, I., Huber, R., Popovic, T.,Turk, V., Towatari, T., Katunuma, N., & Bode, W. (1991) *EMBO J. 10*, 2321−2330.
O'Hara, B. P., Hemmings, A. M., Buttle, D. J., & Pearl, L. H. (1995) *Biochemistry 34*, 13190−13195.
Otwinowski, Z. (1993) in *Data collection and processing* (Sawyer, L., Isaacs, N., & Bailey, S., Eds.) pp 56−62, Daresbury Laboratory, Daresbury, U.K.
Pickersgill, R. W., Goodenough, P. W., Sumner, I. G., & Collins, M. E. (1988) *Biochem. J. 254*, 235−238.
Pickersgill, R. W., Sumner, I. G., Collins, M. E., & Goodenough, P. W. (1989) *Biochem. J. 257*, 309−312.
Pickersgill, R. W., Rizkallah, P., Harris, G. W., & Goodenough, P. W. (1991) *Acta Crystallogr., Sect. B: Struct. Sci. 47*, 766−771.
Pickersgill, R. W., Harris, G. W., & Garman, E. (1992) *Acta Crystallogr., Sect. B: Struct. Sci. 48*, 59−67.
Plou, F. J., Kowlessur, D., Malthouse, J. P. G., Mellor, G. W., Hartshorn, M. J., Pinitglang, S., Patel, H., Topham, C. M., Thomas, E. W., Verma, C., & Brocklehurst, K. (1996) *J. Mol. Biol. 257*, 1088−1111.
Rawlings, N. D., & Barrett, A. J. (1994) *Methods Enzymol. 244*, 461−486.
Revell, D. F., Cummings, N. J., Baker, K. C., Collins, M. E., Taylor, M. A. J., Sumner, I. G., Pickersgill, R. W., Connerton, I. F., & Goodenough, P. W. (1993) *Gene 127*, 221−225.
Riddles, P. W., Blakeley, R. L., & Zerner, B. (1983) in *Methods In Enzymology* (Hirs, C. H., & Timascheff, S. N., Eds.) Vol. 91, pp 49−60, Academic Press, San Diego.
Sakabe, N., Ikemizu, S., Sakabe, K., Higashi, T., Nakagawa, A., Watanabe, N., Adachi, S., & Sasaki, K. (1995) *Rev. Sci. Instrum. 66*, 1276−1281.
Salih, E., Malthouse, J. P. G., Kowlessur, D., Jarvis, M., O'Driscoll, M., & Brocklehurst, K. (1987) *Biochem. J. 247*, 181−193.
Schechter, I., & Berger, A. (1967) *Biochem. Biophys. Res. Commun. 27*, 157−162.
Shipton, M., & Brocklehurst, K. (1978) *Biochem. J. 171*, 385−401.
Sluyterman, L. A. A. E., & Wijdenes, J. (1970) *Biochim. Biophys. Acta 700*, 593−595.
Sumner, I. G., Vaughan, A., Eisenthal, R., Pickersgill, R. W., Owen, A. J., & Goodenough, P. W. (1993) *Biochim. Biophys. Acta 1164*, 243−251.
Taylor, M. A. J., Pratt, K. A., Revell, D. F., Baker, K. C., Sumner, I. G., & Goodenough, P. W. (1992) *Protein Eng. 5*, 455−459.
Taylor, M. A. J., Baker, K. C., Connerton, I. F., Cummings, N. J., Harris, G. W., Henderson, I. M., Jones, S. T., Pickersgill, R. W., Sumner, I. G., Warwicker, J., & Goodenough, P. W. (1994) *Protein Eng. 7*, 1267−1276.
Taylor, M. A. J., Baker, K. C., Briggs, G. S., Connerton, I. F., Cummings, N. J., Pratt, K. A., Revell, D. F., Freedman, R. B., & Goodenough, P. W. (1995) *Protein Eng. 8*, 59−62.
Thomas, M. P., Topham, C. M., Kowlessur, D., Mellor, G. W., Thomas, E. W., Whitford, D., & Brocklehurst, K. (1994) *Biochem. J. 300*, 805−820.
Tipton, K. F., & Dixon, H. B. F. (1983) in *Selected Methods in Enzymology Series* (Colowick, S. P., & Kaplan, O. N., Eds.) pp 97−148, Academic Press.
Topham, C. M., Salih, E., Frazao, C., Kowlessur, D., Overington, J. P., Thomas, M., Brocklehurst, S. M., Patel, M., Thomas, E., & Brocklehurst, K. (1991) *Biochem. J. 280*, 79−92.
Varughese, K. I., Ahmed, F. R., Cary, P. R., Hasnain, S., Huber, C. P., & Storer, A. C. (1989) *Biochemistry 28*, 1330−1332.
Varughese, K. I., Su., Y., Cromwell, D., Hasnain, S., & Xuong, N.-H. (1992) *Biochemistry 31*, 7172−5176.
Vernet, T., Tessier, D. C., Laliberte, F., Dignard, D., & Thomas, D. Y. (1989) *Gene 77*, 229−236.
Vernet, T., Tessier, D. C., Richardson, C., Laliberte, F., Khouri, H. E., Bell, A. W., Storer, A. C., & Thomas, D. Y. (1990) *J. Biol. Chem. 265*, 16661−16666.
Walker, N. C. P., Talanian, R. V., Brady, K. D., Dang, L. C., Bump, N. J., Ferenz, C. R., Franklin, S., Ghayur, T., Hackett, M. C., Hammil, L. D., Herzog, L., Hugunin, M., Houy, W., Mankovich, J. A., McGuinness, L., Orlewicz, E., Paskind, M., Pratt, C. A., Reis, P., Summani, A., Terranova, M., Welch, J. P., Xiong, L., Moeller, A., Tracey, D. E., Kamen, R., & Wong, W. W. (1994) *Cell 78*, 343−352.

BI960949R